Electronic Supplementary Information

Hydration and ion association of La^{3+} and Eu^{3+} in aqueous solution†

Sergej Friesen,[a] Sebastian Krickl,[a] Magdalena Luger,[a] Andreas Nazet,[a] Glenn Hefter[b] and Richard Buchner*[a]

[a] *Institute of Physical and Theoretical Chemistry, University of Regensburg, 93040 Regensburg, Germany. E-mail: richard.buchner@chemie.uni-regensburg.de*

[b] *Chemistry Department, Murdoch University, Murdoch, WA 6150, Australia.*

Supplementary Measurements

Table S1: Concentrations, c, densities, ρ, electrical conductivities, κ, and pH values of investigated aqueous solutions of $LaCl_3$ with ~1 mM HCl(aq) background at 25 °C.

c / M	ρ / g·cm^{-3}	κ / S·m^{-1}	pH
0[a]	0.99708	0.041	3.1
0.03972	1.00605	1.196	3.1
0.06953	1.01276	1.950	3.1
0.1486	1.03011	3.745	3.0
0.2957	1.06230	6.62	2.9
0.4917	1.10456	11.81	2.8
0.7320	1.15464	12.82	2.6
0.9664	1.20492	14.96	2.6

[a] ~ 1mM HCl(aq).

Table S2: Concentrations, c, densities, ρ, electrical conductivities, κ, and pH values of investigated aqueous solutions of $La(NO_3)_3$ with ~1 mM HNO_3(aq) background at 25 °C.

c / M	ρ / g·cm^{-3}	κ / S·m^{-1}	pH
0[a]	0.99709	0.0451	3.0
0.004979	0.99846	0.212	3.0
0.01381	1.00091	0.470	3.0
0.02790	1.00470	0.831	3.0
0.05179	1.01093	1.382	3.0
0.1002	1.02477	2.463	3.0
0.2083	1.05149	4.189	2.9
0.2611	1.06653	5.037	2.9
0.4327	1.10869	6.98	2.8
0.6050	1.15505	8.33	2.7
0.7780	1.19850	9.13	2.6
0.8380	1.21270	9.31	2.6

[a] ~1 mM HNO_3(aq).

Table S3: Concentrations, c, densities, ρ, electrical conductivities, κ, and pH values of investigated aqueous solutions of $La_2(SO_4)_3$ with ~0.5 mM H_2SO_4(aq) background at 25 °C.

c / M	ρ / g·cm^{-3}	κ / S·m^{-1}	pH
0[a]	0.99710	0.0387	3.2
0.00356	0.99925	0.164	–
0.00705	1.00136	0.266	–
0.0106	1.00349	0.358	–
0.0180	1.00770	0.531	–
0.0212	1.00977	0.609	–
0.0283	1.01395	0.766	–
0.0357	1.01799	0.898	2.5

[a] ~0.5 mM H_2SO_4(aq).

Table S4: Concentrations, c, densities, ρ, electrical conductivities, κ, and pH values of investigated aqueous solutions of $Eu(NO_3)_3$ with ~0.225 M HNO_3(aq) background at 25 °C.

c / M	ρ / g·cm^{-3}	κ / S·m^{-1}	pH
0[a]	1.00459	8.48	0.7
0.01551	1.00899	8.73	0.6
0.03083	1.01342	8.97	0.6
0.05379	1.01989	9.22	0.6
0.1147	1.03615	10.05	0.5
0.2276	1.06610	12.33	0.5

[a] ~0.225 M HNO_3(aq).

Table S5: Concentrations, c, densities, ρ, electrical conductivities, κ, and pH values of investigated aqueous solutions of $Eu_2(SO_4)_3$ with ~1 mM H_2SO_4(aq) background at 25 °C.

c / M	ρ / g·cm^{-3}	κ / S·m^{-1}	pH
0[a]	0.99714	0.0822	2.8
0.004001	0.99949	0.155	2.9
0.007966	1.00183	0.211	2.9
0.01194	1.00414	0.261	2.8
0.01492	1.00593	0.298	2.8
0.01787	1.00766	0.331	2.8
0.02086	1.00934	0.360	2.8
0.02490	1.01165	0.407	2.8

[a] ~1 mM H_2SO_4(aq).

Dielectric Spectra and their Fits

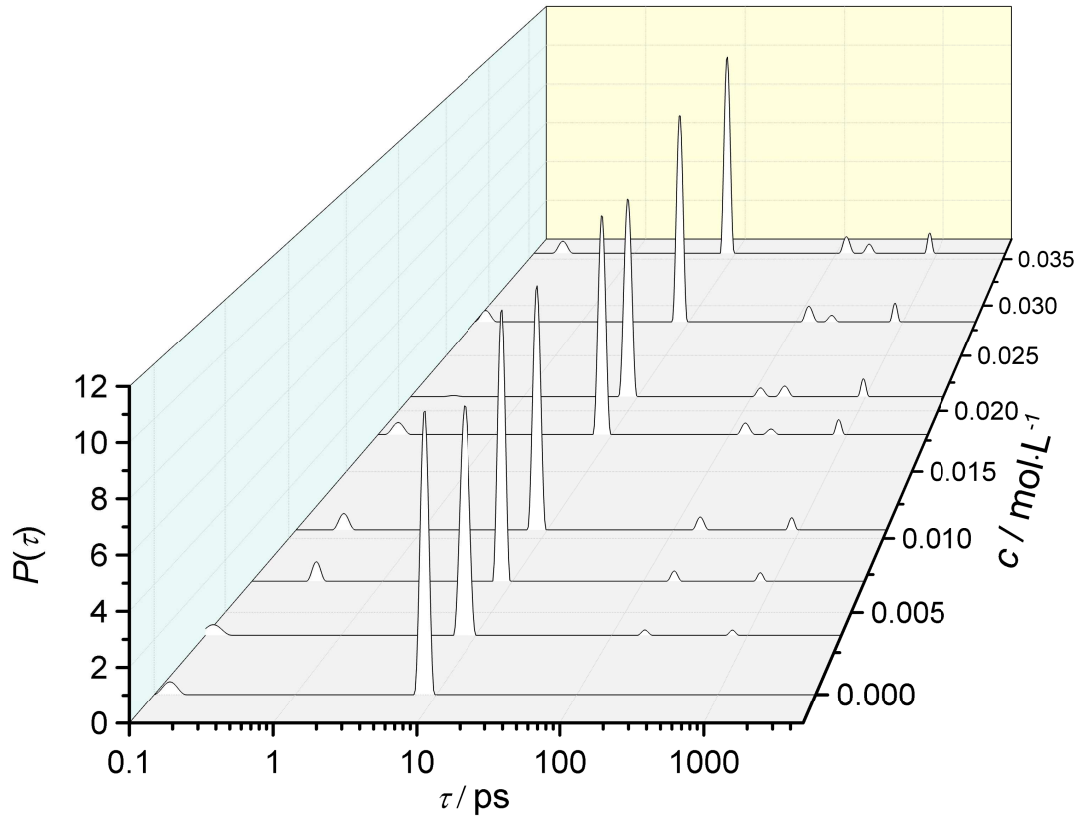

Figure S1: Relaxation-time distribution function, $P(\tau)$, obtained with the method of Zasetsky[1] for the present dielectric spectra of aqueous $La_2(SO_4)_3$ at 25 °C. In addition to the dominant bulk-water contribution at $\tau \approx 8.2$, a peak from fast water at $\tau < 0.4$ ps (too low to be resolved in the fit with Eq. (6) of the Main Manuscript) and two solute-related modes at ~150 ps and ~700 ps are clearly revealed. Due to the small amplitudes of the solute relaxations the suggested splitting of the ~150 ps mode at $c \geq 0.018$ M is too weak to be resolved in a fit with Eq. (6).

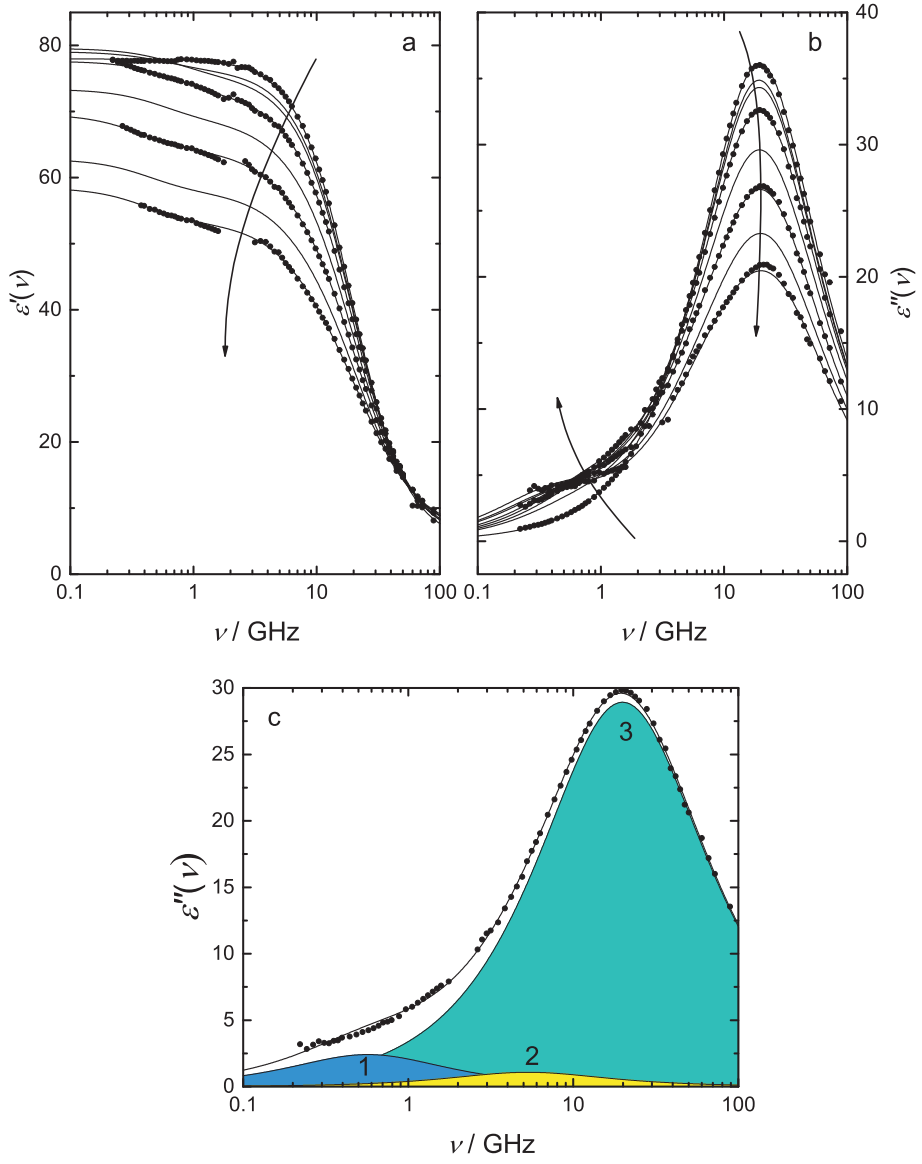

Figure S2: (a) Relative permittivity, $\varepsilon'(\nu)$, and (b) dielectric loss, $\varepsilon''(\nu)$, spectra of $LaCl_3$(aq) at 25 °C and solute concentrations $0 \leq c$ / M ≤ 0.9664. The symbols represent the experimental data (partially omitted for visual clarity) while the lines are fits with a {D}+D+CC model. The arrows indicate the trend in the spectra with increasing c. (c) Dielectric loss, $\varepsilon''(\nu)$, spectrum of $c = 0.2957$ M $LaCl_3$(aq) with shaded areas indicating the resolved modes of a D+D+CC model.

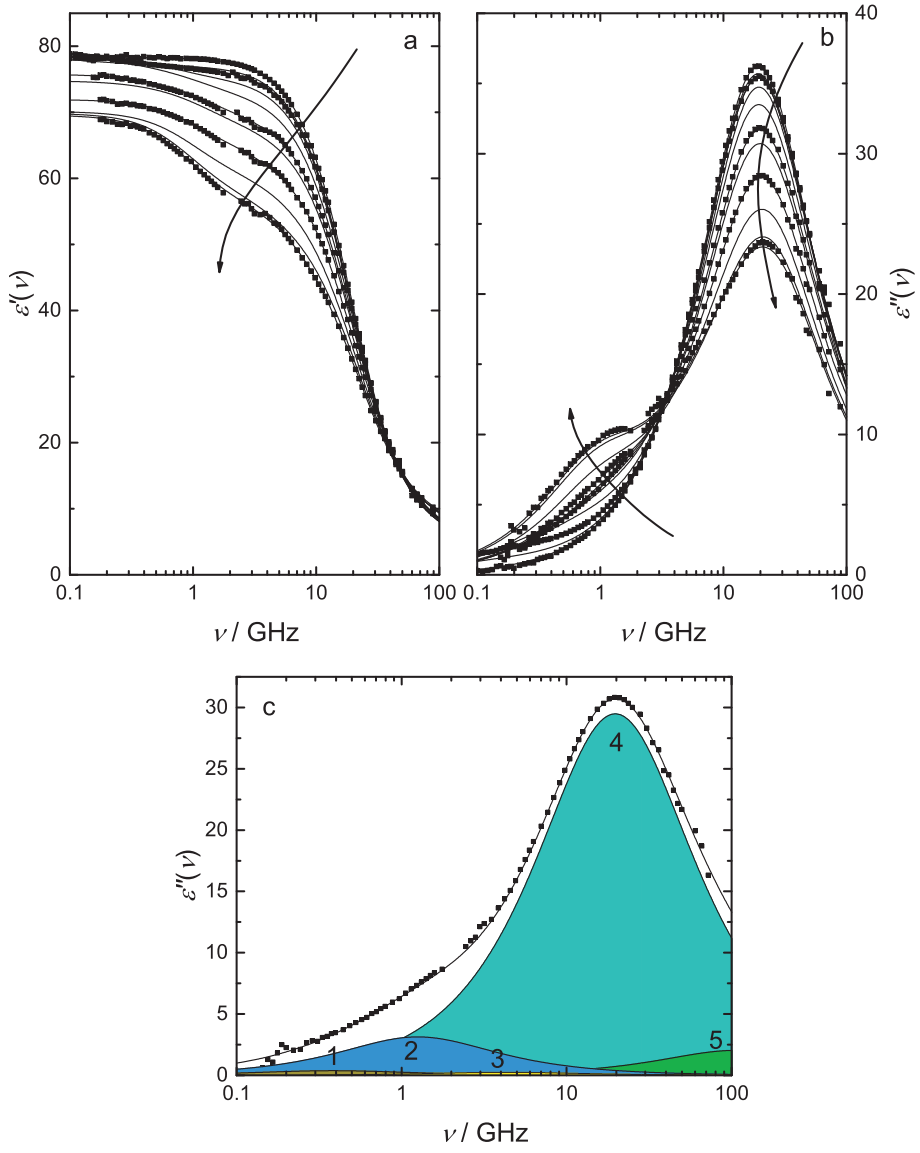

Figure S3: (a) Relative permittivity, $\varepsilon'(\nu)$, and (b) dielectric loss, $\varepsilon''(\nu)$, spectra of $La(NO_3)_3$(aq) at 25 °C and solute concentrations $0 \leq c\,/\,\mathrm{M} \leq 0.8380$. The symbols represent the experimental data (partially omitted for visual clarity) while the lines are fits with a {D}+D+D+D+D model. The arrows indicate the trend in the spectra with increasing c. (c) Dielectric loss, $\varepsilon''(\nu)$, spectrum of $c = 0.2611$ M $La(NO_3)_3$(aq) with shaded areas indicating the resolved modes of a D+D+D+D+D model.

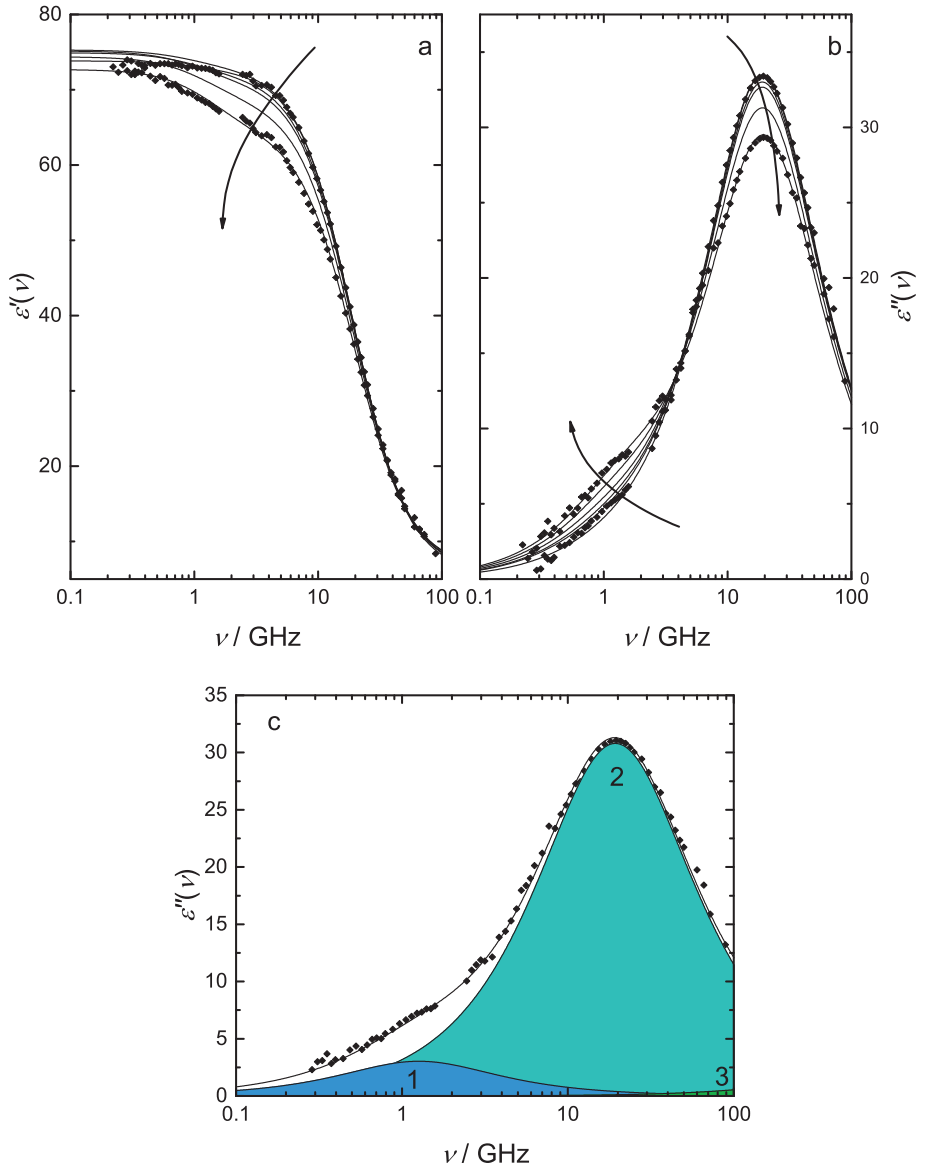

Figure S4: (a) Relative permittivity, $\varepsilon'(\nu)$, and (b) dielectric loss, $\varepsilon''(\nu)$, spectra of $Eu(NO_3)_3$(aq) at 25 °C and solute concentrations $0 \leq c\,/\,\mathrm{M} \leq 0.2276$. The symbols represent the experimental data (partially omitted for visual clarity) while the lines are fits with a D+D+D model. The arrows indicate the trend in the spectra with increasing c. (c) Dielectric loss, $\varepsilon''(\nu)$, spectrum of $c = 0.1147\,\mathrm{M}$ $Eu(NO_3)_3$(aq) with shaded areas indicating the resolved modes of a D+D+D model.

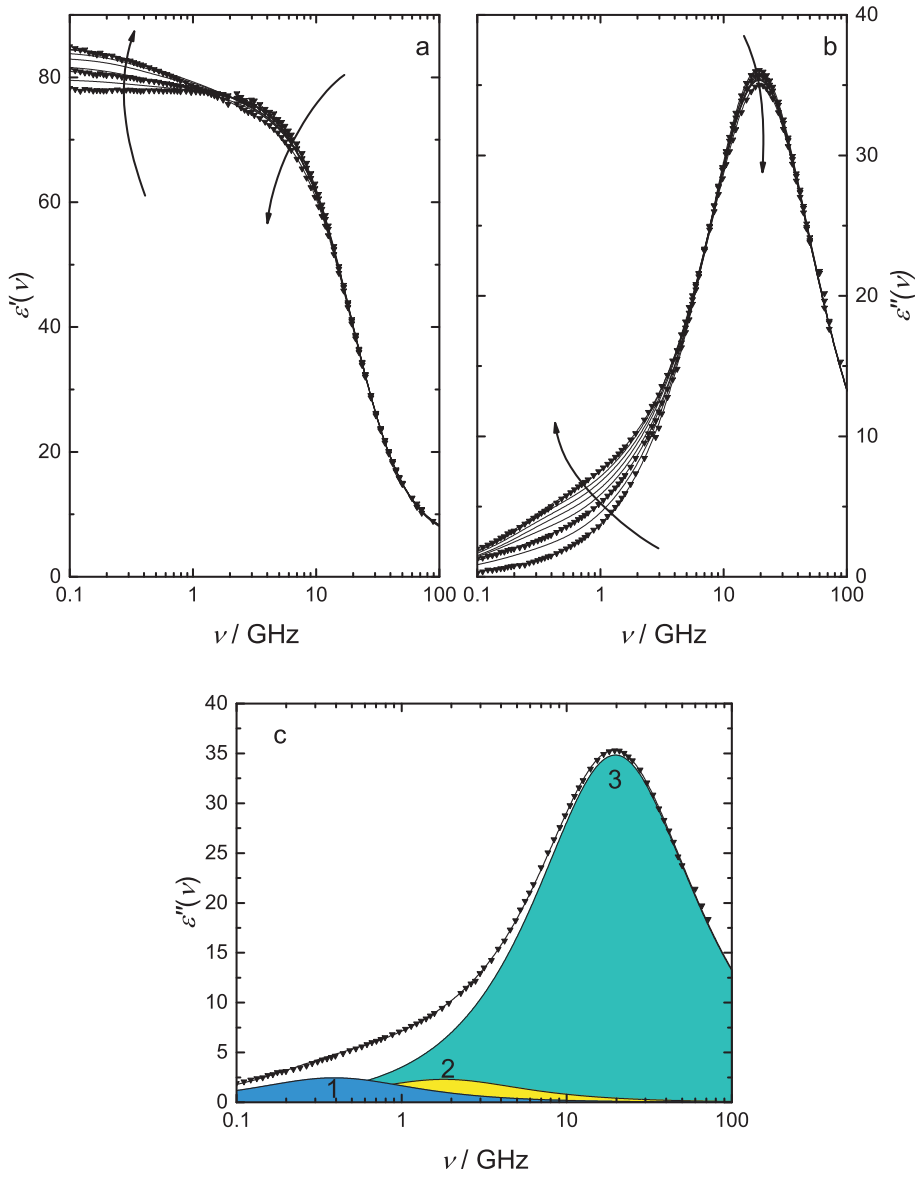

Figure S5: (a) Relative permittivity, $\varepsilon'(\nu)$, and (b) dielectric loss, $\varepsilon''(\nu)$, spectra of $Eu_2(SO_4)_3$(aq) at 25 °C and solute concentrations $0 \leq c\,/\,\mathrm{M} \leq 0.0249$. The symbols represent the experimental data (partially omitted for visual clarity) while the lines are fits with a D+D+D model. The arrows indicate the trend in the spectra with increasing c. (c) Dielectric loss, $\varepsilon''(\nu)$, spectrum of $c = 0.0209$ M $Eu_2(SO_4)_3$(aq) with shaded areas indicating the resolved modes of a D+D+D model.

Table S6: Static permittivity, ε, relaxation amplitudes, S_j ($j = 1 \ldots 3$), relaxation times, τ_j, shape parameter, α_3, and infinite frequency permittivity, ε_∞, of the {D+} D+CC model fitted to the DR spectra of $LaCl_3$(aq) at 25 °C and molar concentration c.[a]

c / M	ε	S_1	τ_1 / ps	S_2	τ_2 / ps	S_3	α_3	τ_3 / ps	ε_∞
0	77.97	–	–	–	–	73.18	0.008	8.20	4.79
0.03972	79.06	2.89	268	–	–	70.54	0.011	8.26	5.43
0.06953	78.85	3.91	171	–	–	69.57	0.012	8.20	5.37
0.1486	77.62	5.08	221	0.84	30F	66.69	0.024	8.14	5.12
0.2957	73.38	4.82	279	2.15	30F	61.19	0.036	8.01	5.22
0.4917	69.58	5.53	436	5.50	29.8	52.53	0.028	7.66	6.02
0.7320	62.78	5.14	366	7.42	22.1	43.97	0.033	7.23	6.25
0.9664	58.44	5.46	387	11.33	19.6	35.07	0.031	6.49	6.58

[a] Parameter values followed by "F" were fixed

Table S7: Static permittivity, ε, relaxation amplitudes, S_j ($j = 1 \ldots 5$), relaxation times, τ_j, and infinite frequency permittivity, ε_∞, of the {D+} D+D+D+D model fitted to the the DR spectra of $La(NO_3)_3$(aq) at 25 °C and molar concentration c.[a]

c / M	ε	S_1	τ_1 / ps	S_2	τ_2 / ps	S_3	τ_3 / ps	S_4	τ_4/ ps	S_5	τ_5 / ps	ε_∞
0	78.30	–	–	–	–	–	–	72.42	8.31	–	–	5.87
0.004979	78.39	0.97	1298	0.38	479	–	–	70.85	8.38	2.40	0.86	3.78
0.01381	79.58	2.08	1103	0.99	283	–	–	69.94	8.38	3.05	1.06	3.52F
0.02790	79.48	2.11	999	0.86	258	–	–	69.94	8.38	3.05	1.06	3.52F
0.05179	79.10	0.71	618	3.31	240	–	–	68.54	8.25	3.71	0.77	2.82
0.1002	78.77	1.79	641	4.31	145	–	–	65.44	8.27	4.76	0.88	2.47
0.2083	75.76	1.28	369	5.35	122	–	–	61.56	8.09	4.05	1.09	3.52F
0.2611	74.77	0.76	415	6.26	127	0.49	37.2	58.95	8.07	4.08	1.47	4.23
0.4327	71.94	–	–	7.51	150	2.96	31.1	53.53	7.69	5.58	0.66	2.36
0.6050	70.14	–	–	9.87	158	4.52	24.4	47.83	7.35	4.41	0.64	3.51
0.7780	69.86	–	–	12.55	169	5.08	29.7	43.82	7.20	4.57	0.68	3.84
0.8380	69.60	–	–	13.37	173	8.61	21.4	39.68	6.77	4.46	0.58	3.48

[a] Parameter values followed by "F" were fixed

Table S8: Static permittivity, ε, relaxation amplitudes, S_j ($j = 1 \ldots 3$), relaxation times, τ_j, and infinite frequency permittivity, ε_∞, of the D+D+D model fitted to the DR spectra of $La_2(SO_4)_3$(aq) at 25 °C and molar concentration c.

c / M	ε	S_1	τ_1 / ps	S_2	τ_2 / ps	S_3	τ_3 / ps	ε_∞
0	77.71	–	–	–	–	72.33	8.21	5.38
0.00356	79.43	0.94	613	1.01	146	72.06	8.19	5.42
0.00705	80.46	1.80	539	1.92	131	71.62	8.14	5.13
0.0106	82.23	2.33	697	3.23	142	71.15	8.17	5.51
0.0180	84.30	3.32	666	4.98	141	70.54	8.15	5.46
0.0212	85.45	3.61	800	6.23	148	70.06	8.18	5.55
0.0283	86.59	4.31	649	7.41	138	69.38	8.16	5.50
0.0357	88.15	5.13	602	8.58	132	68.84	8.15	5.60

Table S9: Static permittivity, ε, relaxation amplitudes, S_j ($j = 1 \ldots 3$), relaxation times, τ_j, and infinite frequency permittivity, ε_∞, of the D+D+D model fitted to the DR spectra of $Eu(NO_3)_3$(aq) at 25 °C and molar concentration c.[a]

c / M	ε	S_1	τ_1 / ps	S_2	τ_2 / ps	S_3	τ_3 / ps	ε_∞
0	73.84	1.22	148	66.65	8.32	2.44	0.28F	3.52F
0.01551	75.29	2.45	161	66.45	8.40	2.88	0.28F	3.52F
0.03083	74.92	3.19	143	65.47	8.31	2.74	0.28F	3.52F
0.05379	75.15	4.19	141	64.66	8.29	2.79	0.28F	3.52F
0.1147	74.38	6.07	126	61.59	8.23	3.20	0.28F	3.52F
0.2276	72.69	8.39	113	57.60	8.03	3.19	0.28F	3.52F

[a] Parameter values followed by "F" were fixed

Table S10: Static permittivity, ε (= $\varepsilon_\infty + \sum S_j$), relaxation amplitudes, S_j ($j = 1 \ldots 3$), relaxation times, τ_j, and infinite frequency permittivity, ε_∞, of the D+D+D model fitted to the DR spectra of $Eu_2(SO_4)_3$(aq) at 25 °C and molar concentration c.[a]

c / mol·dm^{-3}	ε	S_1	τ_1 / ps	S_2	τ_2 / ps	S_3	τ_3 / ps	ε_∞
0	77.92	–	–	–	–	72.17	8.28	5.75
0.004001	79.67	1.40	540F	1.20	90.0F	71.41	8.22	5.66
0.007966	81.15	2.37	503	2.15	90.5	70.95	8.19	5.69
0.01194	81.87	3.02	510	3.16	99.3	70.07	8.13	5.61
0.01492	83.18	3.95	418	3.44	84.6	70.12	8.11	5.67
0.01787	84.10	4.25	433	4.15	94.7	69.94	8.13	5.76
0.02086	84.80	4.91	409	4.60	88.2	69.66	8.07	5.62
0.02490	84.70	5.37	382	5.07	89.9	68.85	8.00	5.41

[a] Parameter values followed by "F" were fixed

Correction for Kinetic Depolarization

Ions moving in an applied electric field exert a torque on neighboring dipolar solvent molecules. This additional force opposes the reorienting force originating from the applied field, $\vec{E}$, resulting in a depolarization of the bulk solvent molecules. Experimentally, this depolarization is expressed as a reduction of the apparent bulk solvent amplitude, S_b^{ap}, by a kinetic dielectric increment, $\Delta\varepsilon_{kd}$. Thus, the corrected equilibrium solvent amplitude, S_b^{eq}, is

$$S_b^{eq} = S_b^{ap} + \Delta\varepsilon_{kd} \tag{1}$$

The continuum model of Hubbard and Onsager[2–4] (HO) is frequently used for the correction of experimental DRS data. In this approach the dielectric increment can be written as

$$\Delta\varepsilon_{kd}^{HO} = p \cdot \frac{\varepsilon(0) - \varepsilon_\infty(0)}{\varepsilon(0)} \cdot \frac{\tau(0)}{\varepsilon_0} \cdot \kappa \tag{2}$$

where ε_0 is the vacuum permittivity, $\varepsilon(0)$ and $\varepsilon_\infty(0)$ are the static and the infinite frequency permittivities of the neat solvent, $\tau(0)$ is the relaxation time of the dominant dispersion step, κ the solution electrical conductivity, and p a hydrodynamic parameter which describes the coupling of ion translational motions to macroscopic viscosity. For $p = 1$, so-called *stick*, and for $p = 2/3$ *slip*, boundary conditions apply. Generally, *slip* conditions are considered as the most physically realistic[5,6] and so were chosen for further analysis since they gave consistent results for limiting ($c \to 0$) hydration numbers of the ions.

Table S11: Effective radii, R, of the ions of the present salts in solution used for the correction of kinetic depolarization.

Salt	$LaCl_3$	$La(NO_3)_3$	$La_2(SO_4)_3$	$Eu(NO_3)_3$	$Eu_2(SO_4)_3$
R / nm	0.286	0.285	0.453	0.280	0.448

The HO theory is only valid at infinite dilution of the electrolyte and thus is problematic for concentrated solutions. Recently, Sega *et al.* introduced a modification of the HO equation to account for finite salt concentrations[7]

$$\Delta\varepsilon_{kd}^{Sega} = \Delta\varepsilon_{kd}^{HO} \cdot \exp(\sigma R) \cdot (\sigma R + 2)/2 \tag{3}$$

where σ is the reciprocal Debye length and R the effective ion radius. Whereas the former quantity can readily be calculated, the determination of the latter is not straightforward. In this work, $R = (r_+ + n \cdot d_w + r_-)/2$ was used for the

effective radius. Here, r_+ and r_- are the the crystallographic radii of the cation and anion,[8] d_w the diameter of a water molecule and n a factor varying from 1 to 2 depending on the present anion. For poorly hydrated Cl^- and NO_3^-, n = 1 was inserted whereas for SO_4^{2-} n = 2 was utilized. The so obtained effective radii are summarized in Table S11.

Coordination Numbers of La^{3+}(aq) and Eu^{3+}(aq)

Table S12: Coordination numbers in the first, CN_1, and second, CN_2, hydration shells of La^{3+} and Eu^{3+} in aqueous solution from literature sources.

cation	CN_1	CN_2
La^{3+}	9[9–16]	11-13[17], 23.4[18], 25.6[19], 15.9[14], 18.8[16],18[12,20]
Eu^{3+}	8-9[10,14,16,20]	15.7[14], 19[16], 18[20]

Determination of Association Constants

Table S13: Calculated effective dipole moments for various types of ion pairs, $\mu_{IP,eff}$, of the studied lanthanide salts in aqueous solution using the CHS model.

	$\mu_{IP,eff}$ / D				
	$LaCl^{2+}$(aq)	$LaNO_3^{2+}$(aq)	$LaSO_4^+$(aq)	$EuNO_3^{2+}$(aq)	$Eu_2SO_4^+$(aq)
CIP	36.3	34.2	41.5	30.9	37.4
SIP	69.1	68.4	81.2	67.2	79.5
2SIP	96.9	96.3	115.7	95.4	114.3

Table S14: Fitting parameters describing the dependence of K_i on I for the present aqueous lanthanide salt solutions at 25 °C.

	$LaCl^{2+}(aq)$		$LaNO_3^{2+}(aq)$		$LaSO_4{}^{+}(aq)$		$EuNO_3^{2+}(aq)$		$Eu_2SO_4{}^{+}(aq)$	
	B	C	B	C	B	C	B	C	B	C
$K_{2SIP}(I)^a$	-0.3 ± 0.1	0.05 ± 0.05^a	-0.83 ± 0.05	0.28 ± 0.02	-6.4 ± 0.3	5.9 ± 0.5	–	–	0.3 ± 0.2	-0.3 ± 0.4
$K_{SIP}(I)^b$	0.14 ± 0.02	–	0.09 ± 0.06	–	0.2 ± 0.1	–	–	–	0 ± 0.1	–
$K_A(I)^a$	-0.35 ± 0.09	0.1 ± 0.03	-0.6 ± 0.1	0.21 ± 0.05	1.4 ± 0.5	-1.3 ± 0.5	-1.6 ± 0.4	0.8 ± 0.3	0.2 ± 0.5	-0.1 ± 0.6

[a] Eq. 14 in the main paper; [b] fitted empirically to $\log K_{SIP}(I) = \log K^{\circ}_{SIP} + B \cdot I$

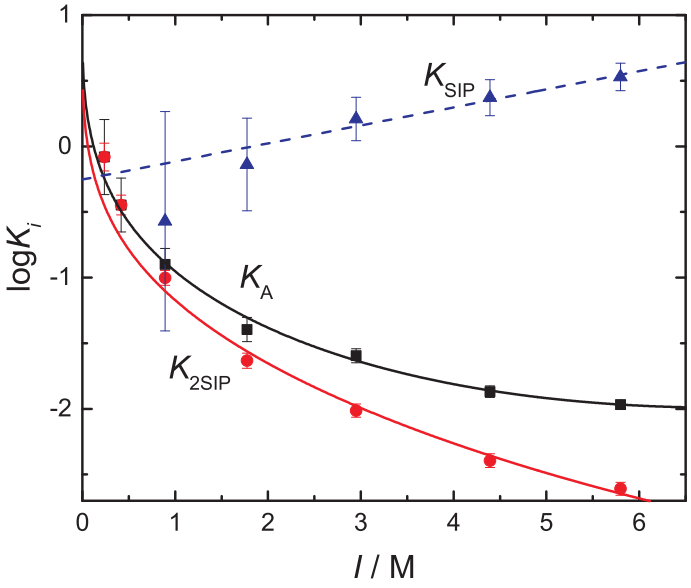

Figure S6: Step-wise formation constants, K_{2SIP} and K_{SIP}, and the overall association constant, K_A, of $LaCl^{2+}$(aq) at 25 °C as a function of the stoichiometric ionic strength, I. Solid lines, Guggenheim-type equation (Eq. 14 main paper); dashed line, empirical straight-line fit.

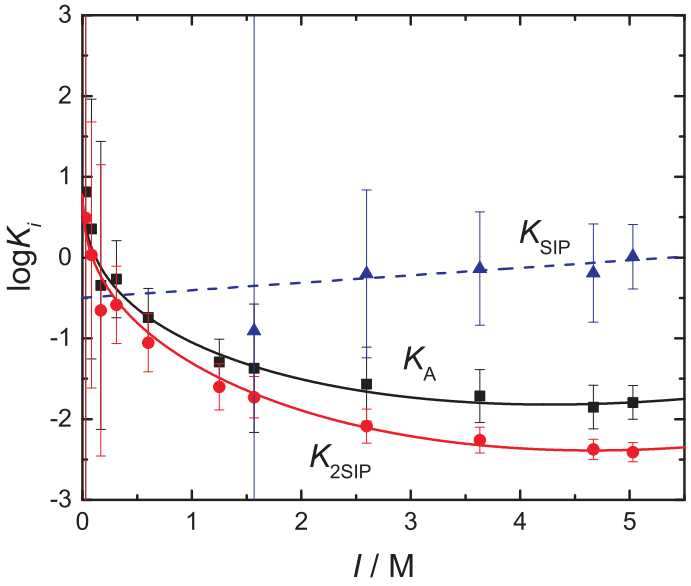

Figure S7: Step-wise formation constants, K_{2SIP} and K_{SIP}, and the overall association constant, K_A, of $LaNO_3^{2+}$(aq) at 25 °C as a function of the stoichiometric ionic strength, I. Solid lines, Guggenheim-type equation (Eq. 14 main paper); dashed line, empirical straight-line fit.

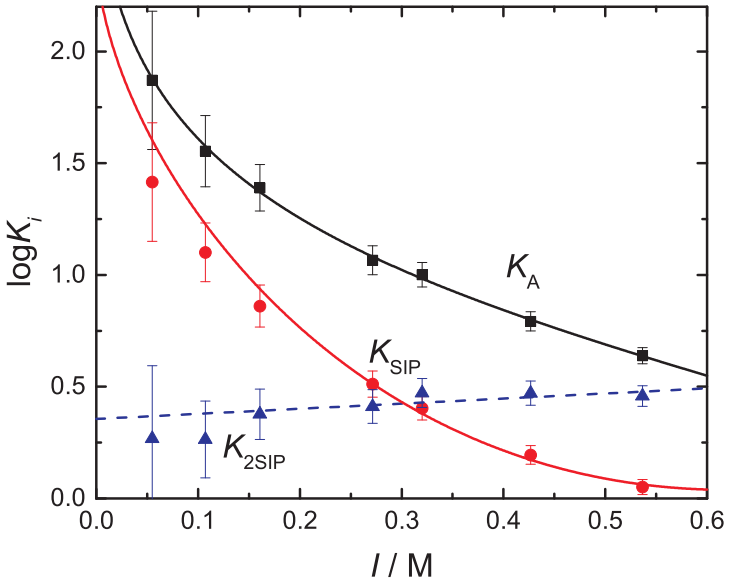

Figure S8: Step-wise formation constants, K_{2SIP} and K_{SIP}, and the overall association constant, K_A, of $LaSO_4^+$(aq) at 25 °C as a function of the stoichiometric ionic strength, I. Solid lines, Eq. Guggenheim-type equation (Eq. 14 main paper); dashed line, empirical straight-line fit.

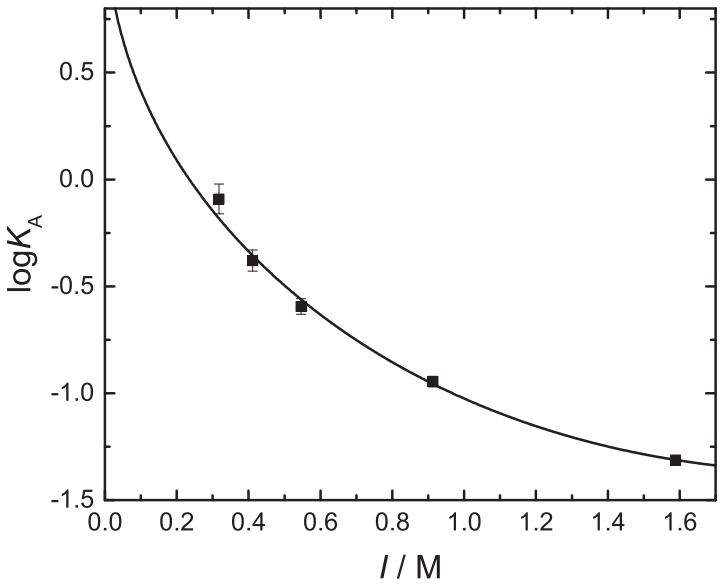

Figure S9: Overall association constant, K_A, of $EuNO_3^{2+}$(aq) at 25 °C as a function of the stoichiometric ionic strength, I.

Bibliography

[1] A. Y. Zasetsky and R. Buchner, *J. Phys.: Condens. Matter*, 2011, **23**, 025903.

[2] J. Hubbard and L. Onsager, *J. Chem. Phys.*, 1977, **67**, 4850–4857.

[3] J. B. Hubbard, *J. Chem. Phys.*, 1978, **68**, 1649–1664.

[4] J. B. Hubbard, P. Colonomos and P. G. Wolynes, *J. Chem. Phys.*, 1979, **71**, 2652–2661.

[5] R. Buchner, T. Chen and G. Hefter, *J. Phys. Chem. B*, 2004, **108**, 2365–2375.

[6] S. Schrödle, W. W. Rudolph, G. Hefter and R. Buchner, *Geochim. Cosmochim. Acta*, 2007, **71**, 5287–5300.

[7] M. Sega, S. Kantorovich and A. Arnold, *Phys. Chem. Chem. Phys.*, 2015, **17**, 130–133.

[8] Y. Marcus, *Ion Properties*, CRC Press, New York, 1997.

[9] H. Grigoriew and S. Siekierski, *J. Phys. Chem.*, 1993, **97**, 5400–5402.

[10] H. Ohtaki and T. Radnai, *Chem. Rev.*, 1993, **93**, 1157–1204.

[11] T. Yamaguchi, M. Nomura, H. Wakita and H. Ohtaki, *J. Chem. Phys.*, 1998, **89**, 5153–5159.

[12] J. Näslund, P. Lindqvist-Reis, I. Persson and M. Sandström, *Inorg. Chem.*, 2000, **39**, 4006–4011.

[13] T. Kowall, F. Foglia, L. Helm and A. E. Merbach, *J. Am. Chem. Soc.*, 1995, **117**, 3790–3799.

[14] C. Clavaguéra, R. Pollet, J. M. Soudan, V. Brenner and J. P. Dognon, *J. Phys. Chem. B*, 2005, **109**, 7614–7616.

[15] M. Duvail, R. Spezia and P. Vitorge, *ChemPhysChem*, 2008, **9**, 693–696.

[16] M. Duvail, P. Vitorge and R. Spezia, *J. Chem. Phys.*, 2009, **130**, 104501.

[17] G. Johansson and H. Wakita, *Inorg. Chem.*, 1985, **24**, 3047–3052.

[18] O. M. Lutz, T. S. Hofer, B. R. Randolf and B. M. Rode, *Chem. Phys. Lett.*, 2012, **536**, 50–54.

[19] T. S. Hofer, H. Scharnagl, B. R. Randolf and B. M. Rode, *Chem. Phys.*, 2006, **327**, 31–42.

[20] P. R. Smirnov and V. N. Trostin, *Russ. J. Gen. Chem.*, 2012, **82**, 360–378.